MASTER OF PHILOSOPHY Modelling of Materials

Examiner's Solutions to Paper 2

SECTION A

1(a)

The hardness of diamond is related to its giant covalent structure, and the need to break the three-dimensional network of strong sp^3 hybridised carbon-carbon bonds.

The malleability of gold is due both to the nature of metallic bonding, which gives rise to a low Peierls-Nabarro stress for dislocation motion, and to its crystalline structure (fcc), which has six independent slip systems (whereas only five are required for general plasticity) along which dislocations can glide.

The electrical conductivity of graphite can be rationalised in two alternative, but essentially equivalent, ways. The first is via the presence of delocalised electron density, due to a p-orbital on each carbon, above and below the plane of the 2-dimensional sp^2 hybridised graphene sheet. The second is to consider the band structure of graphite, which reveals that it is a semi-metal with zero direct band gap at the Fermi level.

1(b)

Lattice type F, motif is S (0,0,0) Zn (¼,¼,¼). There are four formula units (ZnS) in each unit cell (a calculation should involve a consideration of the number of atoms of each type weighted by their contribution to the unit cell). Spacings of the (110) planes in a cubic crystal are given by:

$$d_{110} = \frac{a}{\sqrt{1^2 + 1^2 + 0^2}} = \frac{0.541}{\sqrt{2}} = 0.383 \text{ nm (3 s.f.)}$$

1(c)

The rule of mixtures states that the modulus of the composite E_c, is given by the volume fraction-weighted sum of the moduli of the fibres, E_f, and the matrix, E_m.

$E_c = E_f v_f + E_m v_m$, where $v_f = 1 - v_m$

Hence $E_c = (E_f - E_m)v_f + E_m$

Thus, for the two alternative values of fibre modulus, the volume fractions in an epoxy matrix required to achieve a composite modulus of 80 GPa are given as follows:

$$v_f[1\text{ TPa}] = (E_c - E_m)/(E_f - E_m) = (80-4)/(1000-4) = 0.08$$

$$v_f[100\text{ GPa}] = (E_c - E_m)/(E_f - E_m) = (80-4)/(100-4) = 0.79$$

1(d)

In an electronic structure calculation, Schrödinger's wave equation is traditionally solved by diagonalising the Hamiltonian matrix *H* as shown in the flowchart below. In practice we start with some initial wave functions, generate the charge density, construct and diagonalise *H*, obtain new wave functions and density and repeat the process until the solution is stationary, i.e. density (out) = density (in). This is known as iterating to self-consistency in the electronic density.

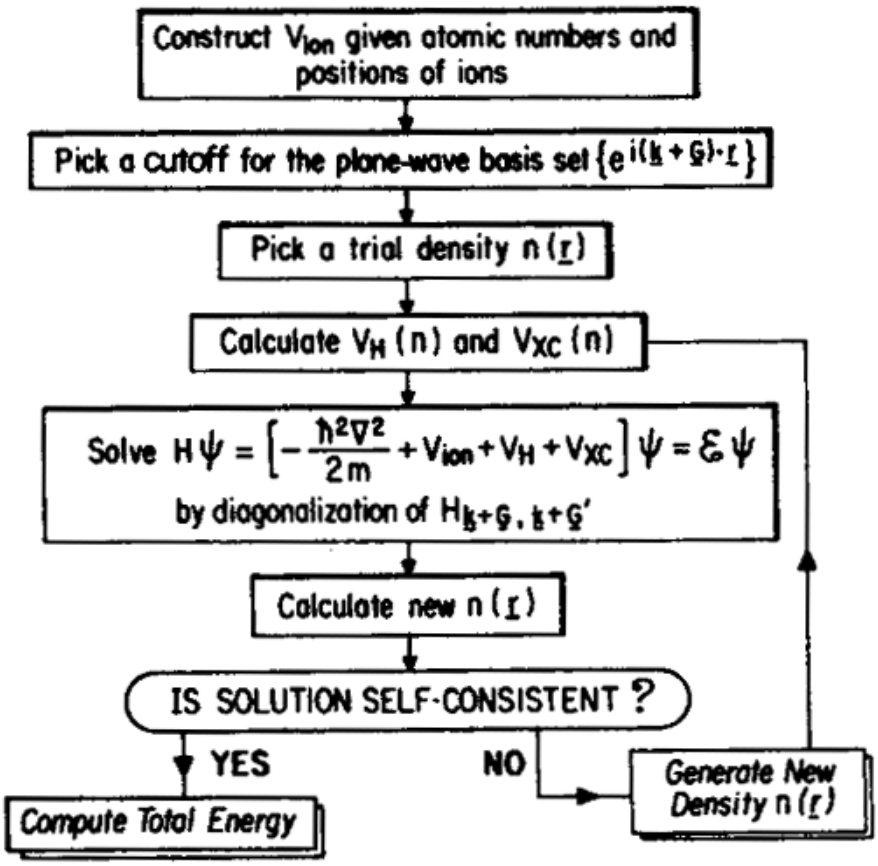

1(e)

An obvious use for a `do` loop would be a simple summation, e.g. $\sum_{i=1}^{3} u_i$,

where the `do`-loop variable *i* would take values from 1 to 3.

However, the application of loops is much wider than this obvious case. `do` loops may be used to repeat an action for all the elements in an array. For example, initialising all the elements to zero; or for performing a matrix multiplication:

$$a_{ij} = \sum_{k=1}^{3} b_{ik} c_{kj}$$

would use `do` loops both to perform the summation over *k*, and to run over all the values of *i* and *j*, setting each element of the product matrix.

An obvious use for `do...while` loops would be in a program employing a numerical technique (such as root-finding) producing successive approximations (say x_n, x_{n+1} and so on) to the result. A `do...while` loop would be used to halt the calculation when succeeding values of x_n were sufficiently close.

1(f)

The mean-square end-to-end distance for a random walk polymer coil is derived as follows:

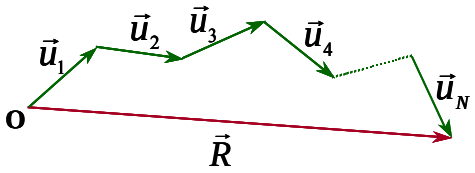

$$R^2 = \left(\sum_{i=1}^{N} \vec{u}_i\right)\left(\sum_{j=1}^{N} \vec{u}_j\right) = \sum_{i=1}^{N}\sum_{j=1}^{N} \vec{u}_i \vec{u}_j$$

$$\left\langle R^2 \right\rangle = \sum_{i=1}^{N}\sum_{j=1}^{N} \left\langle \vec{u}_i \vec{u}_j \right\rangle = \sum_{i=1}^{N} \left\langle \vec{u}_i^2 \right\rangle + \sum_{i=1}^{N}\sum_{j=1}^{N} \left\langle \vec{u}_i \vec{u}_j \right\rangle$$

$$\sum_{i=1}^{N}\sum_{j=1}^{N} \left\langle \vec{u}_i \vec{u}_j \right\rangle = 0 \text{ for random walk, hence } \left\langle R^2 \right\rangle = Nu^2$$

For amino acids, the projected length of monomer in chain direction u will be around 3 Å (a sequence of N-C-C bonds, each of 2 Å, but not in a straight line). Hence: $R \sim 5$ nm, for $N = 300$ as specified in question.

However, the model assumes that monomer segments are uncorrelated in orientation, and have no excluded volume. For this reason, real polymer coils will be 'expanded' compared to the above result, both by local correlations due to main chain stiffness and side groups, and also by long-range correlations due to excluded volume.

1(g)

The definition of thermodynamic temperature is $\frac{1}{T} = \left(\frac{\partial S}{\partial U} \right)_V$, i.e. T is more naturally defined as an inverse quantity $\beta = \left(k_B T \right)^{-1}$ (in units of energy). The latter definition is more consistent with the second and third laws of thermodynamics. That is, negative temperatures, *i.e.* $\beta < 0$, are naturally 'hotter' than positive temperatures, *i.e.* $\beta > 0$, which is what is observed in practice. Furthermore, however much we cool by increasing β, we can never decrease the temperature below absolute zero.

1(h)

A solid particle starts to melt from its surface, which is readily "wetted" by its own melt. Thus, the onset of global melting of a particle is when a spherical solid-liquid interface would start to migrate towards the centre of the particle. This condition for onset is analogous to a critical nucleus of the solid within the liquid. The critical nucleus is in unstable equilibrium with the liquid and, if the temperature is infinitesimally raised, it melts. The unstable equilibrium is at a melt supercooling ΔT inversely proportional to the critical radius r^*. The standard analysis (from classical nucleation theory) gives:

$$r^* = \frac{2\gamma}{\Delta G_V} = 2.5 \text{ nm (for droplet as specified in question)}$$

from which follows:

$$\Delta G_V = \frac{2\gamma}{r^*} = \frac{2 \times 0.3}{2.5 \times 10^{-9}} = 2.4 \times 10^8 \text{ J m}^{-3}$$

The driving free energy for solidification (per unit volume), ΔG_V, is given by the following expression:

$$\Delta G_V = \Delta S_V \Delta T = \frac{\Delta H_V}{T_m}\Delta T \quad \text{(derived by setting } \Delta G = 0 \text{ at } T = T_m\text{)}$$

Thus, the supercooling ΔT is given by:

$$\Delta T = \frac{T_m \Delta G_V}{\Delta H_V} = \frac{1337 \times 2.4 \times 10^8}{1.25 \times 10^9} = 257 \text{ K}.$$

Hence, the melting temperature T' = 1337 – 257 = 1080 K.

1(i)

Conventional error minimisation identifies an optimum set of parameters. Students are expected to quote Bayes' theorem in the form below, and identify *prior*, $P(\Theta|H)$, *likelihood*, $P(D|\Theta,H)$, *evidence,* $P(D|H)$ and the *posterior*, $P(\Theta|D,H)$, distributions. The method allows one to fit a probability distribution of the adjustable parameters (or weights). If different values of the weights have similar, high probabilities (i.e. a wide distribution) then different predictions will also have reasonably high probabilities, i.e. the error bars will be large. If on the contrary, there are sufficient data and the posterior probability is narrow around the optimum values, then the error bars will be small.

$$P(\Theta \mid D,H) = \frac{P(D \mid \Theta,H)P(\Theta \mid H)}{P(D \mid H)}$$

1(j)

Limit analysis is used in plastic deformation situations to specify either minimum loads below which something will definitely not deform plastically (lower bound solutions) or loads for which plastic deformation is guaranteed (upper bound solutions). Thus, lower bound solutions are definite underestimates of the load required to cause plastic deformation, while upper bound solutions are definite overestimates of the same load.

For the notched metallic bar in plane strain tension, a suitable lower bound estimate can be found by invoking a suitable stress system, for

example one where the stress over the projected area containing the notch is zero, and the stress is equal to the yield stress elsewhere.

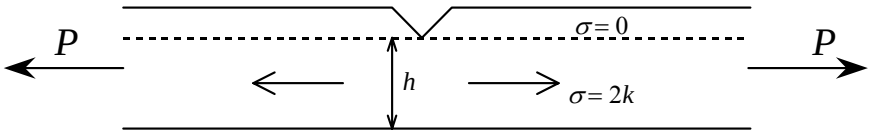

For plane strain deformation where one principal stress within the plane is zero, the uniaxial yield stress at which plastic deformation begins is $2k$, where k is the shear yield stress.

Hence, for a slab of breadth b, we can equate forces to show that:

$$P = 2\,k\,b\,h$$

is our maximum estimate of the lower bound load required to just cause plastic deformation of the notched bar.

An upper bound estimate can be found by assuming that plastic deformation occur by shear yielding on two planes AB and AC at 45° to the uniaxial tensile stress.

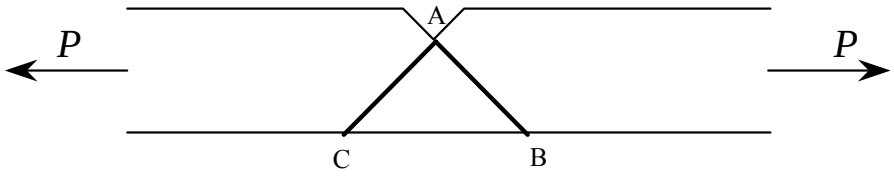

Suppose shear yielding causes a displacement δx along AB. The component of this displacement parallel to the uniaxial tensile stress is:

$$\delta x \cos 45^\circ = \frac{\delta x}{\sqrt{2}}$$

The length AB = $\sqrt{2}h$. Hence the work done within the metal shearing a distance δx along AB, W_{internal}, is:

$$W_{\text{internal}} = kbh\sqrt{2}\delta x$$

since the area over which the shear stress acts is $b\sqrt{2}h$. If the process is 100% efficient, so that there is no heat lost during the process, this must be equal to the external work done moving through a distance δx cos 45°, W_{external}.

Therefore, in general,

$$P\frac{\delta x}{\sqrt{2}} \geq kbh\sqrt{2}\delta x$$

with equality when the process is 100% efficient – this will be the lowest value we can obtain for our upper bound solution. Hence the minimum value of the upper bound solution that we obtain for P is:

$$P = 2\,k\,b\,h$$

which for this particular case is the same as the lower bound solution.

Thus, in this very special case, we can be confident that we have found the exact load necessary to cause plastic deformation to occur.

SECTION B

2.

The density of allowed states is defined as the number of electron states *N(E)* per unit energy range and given mathematically by $D(E) = \frac{dN(E)}{dE}$. Note that a state is defined by both a level and a spin. The number of states is equal to twice the number of levels due to the Pauli exclusion principle.

At $T = 0$, the allowed states are fully occupied below the Fermi energy and completely unoccupied above the Fermi energy.

At $T > 0$, the probability $F(E)$ that an electron state at energy E will be occupied is determined by Fermi-Dirac statistics. The probability function is given by:

$$F(E) = \frac{1}{1 + e^{(E-E_F)/kT}} \quad \text{where } E_F \text{ is the Fermi energy.}$$

Therefore the density of occupied states at $T > 0$ is given by:

$$Z(E) = D(E)F(E)$$

[20%]

(i) Consider free electrons in a '1-D box' of length *L*.

In k-space, equal values of electron energy E lie at the end of a line of length k.

Number of electrons along line: $N = \frac{2 \times \text{length of line}}{\text{length per k-state}}$ (including spin).

Length per k-state $= \frac{2\pi}{L}$.

Therefore $N = \frac{k}{2\pi/L} 2 = \frac{Lk}{\pi}$.

Thus $N = \frac{L}{\pi}\left(\frac{2mE}{\hbar^2}\right)^{1/2}$ since $E = \frac{\hbar^2 k^2}{2m}$.

Note that the number of electrons N equals the number of states.

$$\text{Hence } D(E) = \frac{dN(E)}{dE} = \frac{L}{2\pi}\left(\frac{2m}{\hbar^2}\right)^{1/2} E^{-1/2}$$

Sketch of *D(E)*

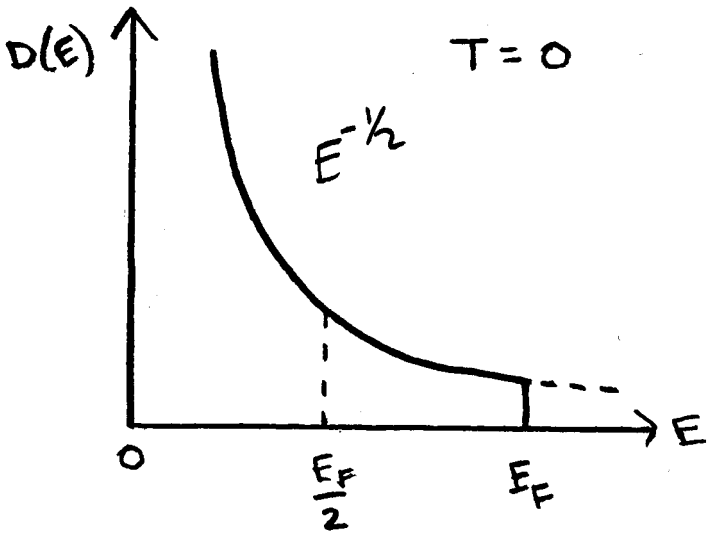

[20%]

(ii) Fraction of free electrons with energies above $E_F/2$ is given by:

$$\frac{\int_{E_F/2}^{E_F} E^{-1/2}dE}{\int_0^{E_F} E^{-1/2}dE} = \frac{2E_F^{1/2} - 2(E_F/2)^{1/2}}{2E_F^{1/2}} = 1 - \frac{1}{\sqrt{2}} = 0.29$$

[10%]

(iii) For a 2-D metal *D(E)* = constant, *A* say. Therefore the fraction of free electrons with energies above $E_F/2$ is given by:

$$\frac{\int_{E_F/2}^{E_F} AdE}{\int_0^{E_F} AdE} = \frac{E_F - (E_F/2)}{E_F} = 0.50$$

[10%]

(iv) Sketch of the occupation density of states for a 1-D free electron metal at $T > 0$:

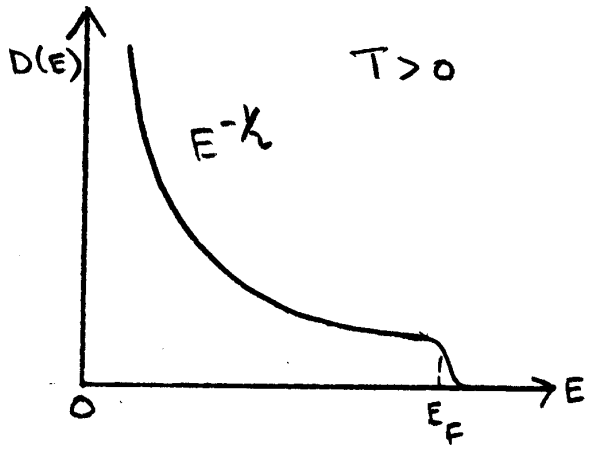

[20%]

(v) Sketch of the allowed density of states for a 1-D *nearly free electron metal*

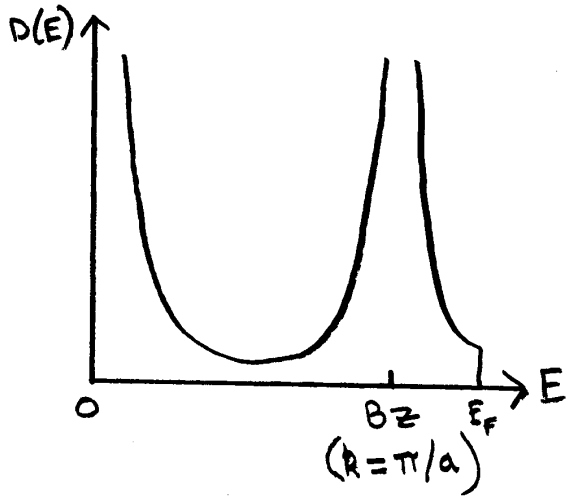

$$D(E) = \frac{dN(E)}{dE} = \frac{dN}{dk} \Big/ \frac{dE}{dk}$$

When the lattice potential is weak $\frac{dE}{dk} \to 0$ at $k = \frac{n\pi}{a}$, where a is the lattice constant. In the Ziman model, travelling waves become standing waves with zero group velocity (the gradient of the E-k curve). Thus $D(E) \to \infty$ at the Brillouin Zone (BZ) boundaries, as shown above. These discontinuities become van Hove singularities in a 3-D crystal.

[20%]

3.

If the chemical potential of the solute is known, and the solution is an ideal solution (no solute-solute interactions), then the change in surface tension γ may be related to the concentration of the solute by the following argument.

Starting with master equation for Gibbs free energy:

$$\mathrm{d}G = -S\mathrm{d}T + V\mathrm{d}p + \sum_i \mu_i \mathrm{d}n_i + \gamma \mathrm{d}A$$

where S, T, V and p have their usual meanings, μ_i and n_i are the chemical potential and number of species i, γ is the surface tension and A is the area of interface between the components.

The full master equation simplifies at constant T and p to:

$$\mathrm{d}G = \sum_i \mu_i \mathrm{d}n_i + \gamma \mathrm{d}A \qquad (1)$$

Integrating both sides, $G = \sum_i \mu_i n_i + \gamma A$, and then differentiating fully:

$$\mathrm{d}G = \sum_i \mu_i \mathrm{d}n_i + \sum_i n_i \mathrm{d}\mu_i + \gamma \mathrm{d}A + A\mathrm{d}\gamma \qquad (2)$$

Comparing the forms of equations (1) and (2), it is clear that:

$$\sum_i n_i \mathrm{d}\mu_i + A\mathrm{d}\gamma = 0 .$$

Hence, defining n_i/A as the surface excess Γ_i, then:

$$\mathrm{d}\gamma = -\sum_i \Gamma_i \mathrm{d}\mu_i \text{ , and since } \mu_i = RT \ln C_i \Rightarrow \mathrm{d}\mu_i = RT\mathrm{d}\ln C_i$$

then $\mathrm{d}\gamma = -RT \sum \Gamma_i . \mathrm{d}\ln C_i$, which was the result to be proved.

[40%]

Using the Gibbs adsorption isotherm,

$$\mathrm{d}\gamma = -RT\sum \Gamma_i . \mathrm{d}\ln C_i$$

and setting the surface excess of component A to zero, then:

$$\mathrm{d}\gamma = -RT\Gamma_\mathrm{B}\mathrm{d}\ln C_\mathrm{B} \qquad (*)$$

Differentiating with respect to C_B yields:

$\gamma = -\gamma_\mathrm{A} - b\gamma_\mathrm{A}\ln\left(1 + C_\mathrm{B}/a\right)$, i.e. Szyszkowski relation given in question.

Differentiating again with respect to C_B yields:

$$\begin{aligned}\mathrm{d}\gamma &= \mathrm{d}\gamma_\mathrm{A} - \mathrm{d}\left\{b\gamma_\mathrm{A}\ln\left(1 + C_\mathrm{B}/a\right)\right\} \\ &= 0 - \frac{b\gamma_\mathrm{A}}{a}\frac{1}{1 + C_\mathrm{B}/a}\end{aligned}$$

using the lemma given that $\dfrac{\mathrm{d}}{\mathrm{d}C_\mathrm{B}}\left\{\ln\left(1 + C_\mathrm{B}/a\right)\right\} = \dfrac{1}{1 + C_\mathrm{B}/a}\dfrac{\mathrm{d}\left(1 + C_\mathrm{B}/a\right)}{\mathrm{d}C_\mathrm{B}}$.

However, $\dfrac{\mathrm{d}\ln C_\mathrm{B}}{\mathrm{d}\gamma} = \dfrac{1}{C_\mathrm{B}}\dfrac{\mathrm{d}C_\mathrm{B}}{\mathrm{d}\gamma} = -RT\Gamma_\mathrm{B}$ from equation (*), and so:

$$C_\mathrm{B}\frac{\mathrm{d}\gamma}{\mathrm{d}C_\mathrm{B}} = -RT\Gamma_\mathrm{B}$$

$$C_\mathrm{B}\frac{b\gamma_\mathrm{A}}{a}\frac{1}{1 + C_\mathrm{B}/a} = RT\Gamma_\mathrm{B}$$

Setting $\Gamma_\mathrm{B}^\infty \equiv b\gamma_\mathrm{A}/RT$ and $\alpha \equiv 1/a$, we obtain:

$$\alpha C_\mathrm{B}\Gamma_\mathrm{B}^\infty\frac{1}{1 + \alpha C_\mathrm{B}} = \Gamma_\mathrm{B} \Rightarrow \Gamma_\mathrm{B} = \Gamma_\mathrm{B}^\infty\left\{\frac{\alpha C_\mathrm{B}}{1 + \alpha C_\mathrm{B}}\right\}$$

which was the result to be proved (note that this has the same form as the Langmuir isotherm).

[60%]

4.

In many designs, the combination of material properties can maximise performance of a component. For example, the expression for the maximum stiffness and minimum weight of a rod subjected to tensile loading or bending will include the a term of the form E^n/ρ where E is the Young's modulus, ρ is the density of candidate materials and n is a constant with a numerical value depending on the precise loading conditions.

Materials selection charts show relationships between two (or more) properties by plotting graphically the values of the properties, generally on a logarithmic scale. Hence the above example provides an expression of the form $n\log E = \log \rho$. This expression can be plotted on a materials selection chart as a series of lines all with gradient n.

All materials on a given line have the same value of E^n/ρ and hence will behave similarly. Materials above the line and to the top left-hand corner in figure 2 in question paper, have the potential to be the stiffest and lightest; hence would be good choices for the application outlined above.

Elastic energy per unit volume can be determined in **either** of two ways (give equal credit):

a)

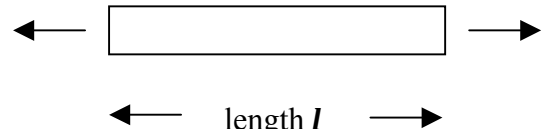

$\sigma = E\,\varepsilon \quad \Rightarrow \quad F/A = E\,e/l \quad \Rightarrow \quad F = (EA/l)\,e$ **or** $F = k\,e$

Stored energy $= \int F\,de = \int k\,e\,de = \tfrac{1}{2} k\,e^2 = \tfrac{1}{2} F^2/k$
$= \tfrac{1}{2}\sigma^2 A^2/k = \tfrac{1}{2}\sigma^2 A^2/(E\,A/l)$

Stored energy / unit volume $= [\tfrac{1}{2}(\sigma^2 A^2 l)/(E\,A)]/[A\,l] = \tfrac{1}{2}\sigma^2/E$

b) Directlv from stress-strain curve

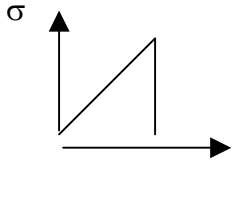

Stored energy is area under elastic region of stress/strain Plot
$= \tfrac{1}{2}\sigma\,\varepsilon = \tfrac{1}{2}\sigma^2/E$

Hence to maximise energy stored per unit volume, need to consider merit index of σ^2/E. Use Modulus – strength (yield) selection chart provided in question paper (figure 2)

Need to choose materials in bottom right-hand corner to maximize energy stored, and then move a line of gradient 2 (shown by guide line $\sigma^2/E\rho$ = constant), which denotes equivalent materials, to the left.

Other properties include fracture toughness mainly. Also have to consider actual constraints associated with particular use of spring, hence often specify a minimum strength since many applications will require spring not to plastically yield.

In practice, low fracture toughness will eliminate many ceramics – materials in top right hand corner. Then materials on a line of gradient 2 will be appropriate depending on the minimum strength required. Suggest steels, glass or carbon fibre reinforced polymers (CFRP, GFRP), or even elastomers (but these generally will have too low yield strengths for most applications).

Elastic energy per unit mass can be determined using density ρ = mass /volume

Hence merit index to maximize energy per unit mass = merit index per unit volume / ρ

$$= \sigma^2/(\rho E)$$

$$= (\sigma/\rho)^2/(E/\rho)$$

Use Specific Modulus – Specific strength (yield) selection chart provided.

Alters selection in that steels now less favourable compared with CFRP, GFRP, and also engineering polymers now of greater interest.

For the following applications:

(a) spring used as part of a car suspension system – steel due to need for minimal strength

(b) a non-metallic torsional spring in the form of a long thread/fibre – polymer (e.g. nylon) or glass (both easy to fabricate in right shape)

(c) the locking catch on a food container – polypropylene since likely to be integral to box

5.

The Frisch Hasslaucher Pomeau (FHP) lattice gas model is constructed of discrete, identical particles that move from site to site on a triangular lattice, colliding when they meet, always conserving particle number and momentum. FHP showed that it is possible to derive the Navier-Stokes equations from the micro dynamics of this system. The innovative feature of FHP model is the simultaneous discretisation of space, time, velocity and density. No more than one particle may reside at a given site and move with a given velocity. Unlike purely diffusive lattice gases, momentum is conserved in each collision and so the system is Galilean invariant and therefore displays hydrodynamic behaviour. Unlike the hydrodynamic lattice gas models that preceded it, the FHP model has an isotropic hydrodynamic limit because of the underlying symmetry of the triangular lattice. Three examples of its application would be to modelling flow of immiscible binary liquids (e.g. oil/water), as an alternative to mesh-based computational fluid dynamics, and modelling flow through porous media.

[20%]

The microdynamics of the FHP lattice gas model are described by the following equation:

$$n_i(\mathbf{x}+\mathbf{c}_i, t+1) = n_i(\mathbf{x}, t) + \Delta_i\left[n(\mathbf{x}, t)\right] \qquad (*)$$

where n_i are the particle fluxes from site $\mathbf{x}$ to site $\mathbf{x} + \mathbf{c}_i$ on the lattice, $\mathbf{x}$ are position vectors of the lattice sites, $\mathbf{c}_i$ are translation vectors between adjacent lattice sites, $\mathbf{c}_i = (\cos \pi i/3, \sin \pi i/3)$ [where i = 1, 2, … , 6], t is the time (a discrete variable) and Δ_i is the collision operator.

The collision operator, Δ_i, describes the change in fluxes n_i due to particle collisions and takes values ±1 or 0. In the original FHP algorithm, it is the sum of two Boolean expressions for the two-body and three-body collisions. More elaborate collision operators may be formed by including four-body collisions or "rest" particles, but these are beyond the scope of the question. Whatever its form, there are two restrictions on Δ_i, namely that it conserve mass and momentum for each flux:

i.e. $\sum_i \Delta_i(\mathbf{n}) = 0$ and $\sum_i \mathbf{c}_i \Delta_i(\mathbf{n}) = 0$.

This is necessary for the FHP model to reproduce the correct hydrodynamic behaviour of the system.

Summing the microdynamical equations of motion (*) over all lattice sites, and imposing the two constraints on the collision operator, we can obtain the mass and momentum balance relations for the system as follows:

$$\sum_i n_i(\mathbf{x}+\mathbf{c}_i, t+1) = \sum_i n_i(\mathbf{x},t) + \sum_i \Delta_i\left[n(\mathbf{x},t)\right]$$
$$= \sum_i n_i(\mathbf{x},t)$$

for mass balance at each time step.

$$\sum_i \mathbf{c}_i n_i(\mathbf{x}+\mathbf{c}_i, t+1) = \sum_i \mathbf{c}_i n_i(\mathbf{x},t) + \sum_i \mathbf{c}_i \Delta_i\left[n(\mathbf{x},t)\right]$$
$$= \sum_i \mathbf{c}_i n_i(\mathbf{x},t)$$

for momentum balance at each time step.

Hence mass and momentum are conserved throughout the simulation at each time step.

[50%]

The FHP model can be considered deficient over continuum methods for modelling flow, such as finite element or smoothed particle hydrodynamic methods for solving Navier-Stokes equations, mainly because of the level of noise inherent in having Boolean occupancies at each lattice site. This means that to obtain meaningful information about fluid densities and velocities at each point, one must average over long times in order to produce an acceptably low level of signal-to-noise. The extra computation required acts partially to offset the intrinsic efficiency of the FHP algorithm itself, although it is still considerably more robust than mesh-based methods when there are large variations in fluid velocity or density. In addition, FHP LG simulations in 3D are complicated by the fact that there is no 3D lattice with an isotropic hydrodynamic limit, i.e. there will always be preferred directions for fluid flow. To get around this, one must carry out LG simulations in an isotropic 4D lattice and project the results back into 3D space, which again results in additional computational overhead compared to more conventional CFD methods.

[30%]

6.

An equation of state relates the pressure, volume and temperature of a system in thermal equilibrium. A simple example of an equation of state that is applicable to non-interacting particles in the gas phase is the *ideal gas* equation: $pV = nRT$, where p is the pressure, V is the volume, n is the number of moles of ideal gas, R is the molar gas constant (8.314 J K^{-1} mol^{-1} in conventional units) and T is the temperature. This equation is obeyed quite well for most gases at room temperature and pressure, and increasingly so as the pressure is decreased. However, at higher pressures and lower temperatures, interactions between the gas molecules become significant, and so a more complicated equation of state is required.

[10%]

The canonical ensemble is defined by constant particle number, constant volume and constant temperature (NVT). In order to generate system configurations in the NVT ensemble, the standard constant energy (microcanonical) molecular dynamics algorithm must be modified so that particles can exchange thermal energy with a reservoir and thereby come to thermal equilibrium. Standard microcanonical MD solves Newton's equations of motion with forces calculated from the derivative of the potential energy of the system (force field) using a finite-difference integration method. However, in canonical MD, these forces are supplemented by fictitious forces representing the exchange of energy with the reservoir at constant temperature. A convenient way to calculate the forces required to achieve constant temperature is to use an extended Lagrangian, which includes an extra coordinate ζ that evolves in time so as to minimise the difference between the instantaneous kinetic and statistical temperatures. The modified equations of motion become:

$$\dot{\mathbf{r}}_i = \mathbf{p}_i / m_i$$
$$\dot{\mathbf{p}}_i = \mathbf{F}_i - \zeta \mathbf{p}_i$$
$$\dot{\zeta} = \frac{1}{\tau_T^2}\{T_K(t)/T_S - 1\}$$

where $\mathbf{r}_i$ are the particle positions (with dotted quantities being the time derivatives), $\mathbf{p}_i$ are the particle momenta, m_i the particle masses, $\mathbf{F}_i$ the forces on particles arising from the derivative of the potential energy, τ_T being the thermostat relaxation time, T_K the instantaneously measured kinetic temperature (relative to average kinetic energy of particles) and T_S is the statistical temperature (a simulation parameter).

A plot of the simulated data (V,p) for the van der Waals gas reveals the location of the point of inflection at T = 150 K.

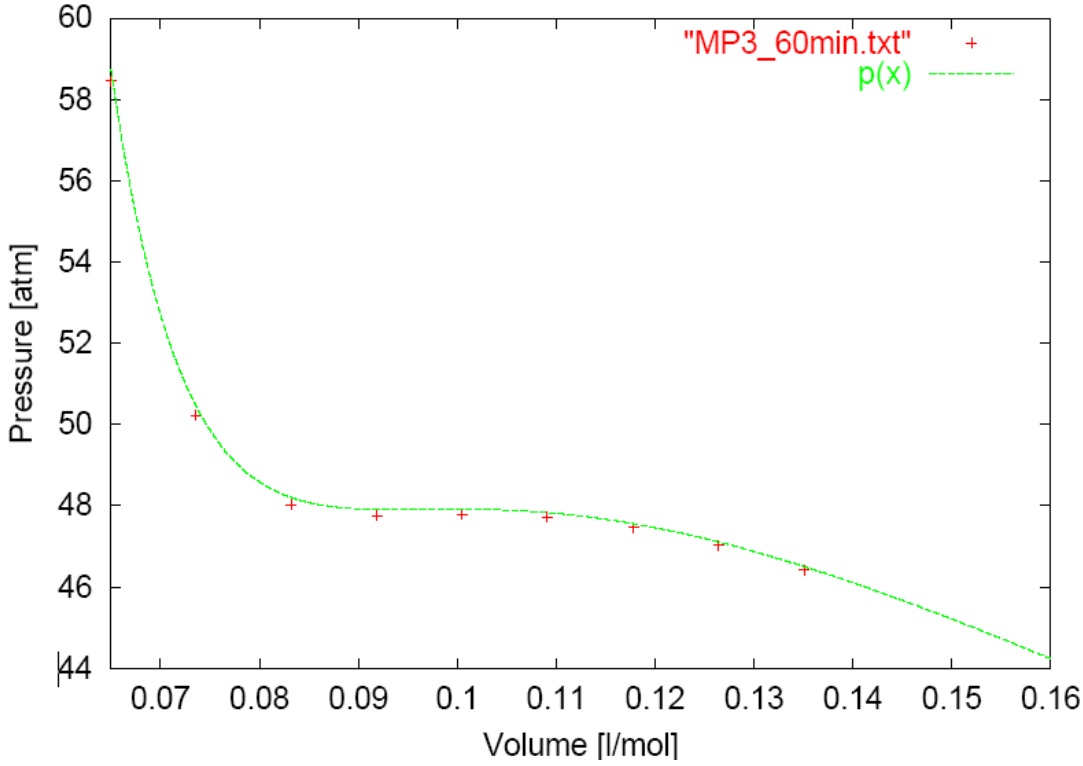

The position of the point of inflection at (0.096,48), hence the parameters a and b, can be found directly from the equation of state (*) by differentiation.

$$p = \frac{RT}{(V_m - b)} - \frac{a}{V_m^2} \qquad (*)$$

$$\left.\begin{aligned} \frac{\mathrm{d}p}{\mathrm{d}V_\mathrm{m}} &= \frac{-RT}{(V_\mathrm{m} - b)^2} + \frac{2a}{V_\mathrm{m}^3} = 0 \\ \frac{\mathrm{d}^2 p}{\mathrm{d}V_\mathrm{m}^2} &= \frac{2RT}{(V_\mathrm{m} - b)^3} - \frac{6a}{V_\mathrm{m}^4} = 0 \end{aligned}\right\} \text{ at } p_\mathrm{c},\, V_\mathrm{c},\, T_\mathrm{c}$$

Hence, separating terms to opposite sides of the equality and dividing:

$$\frac{RT}{(V_\mathrm{c} - b)^2} \frac{(V_\mathrm{c} - b)^3}{2RT} = \frac{2a}{V_\mathrm{c}^3} \frac{V_\mathrm{c}^4}{6a}$$

$$\therefore \frac{3(V_c - b)}{2} = V_c \Rightarrow V_c = 3b \qquad \therefore b = V_c / 3$$

$$\therefore p_c = \frac{RT_c}{2b} - \frac{a}{9b^2} \Rightarrow p_c = \frac{9RbT_c - 2a}{18b^2} \qquad \therefore a = \frac{9b}{2}(RT_c - 2bp_c)$$

From graph above, $V_c \approx 0.096$ dm^3 mol^{-1} and $p_c \approx 48$ atm, which yield the following values of a and b when substituted into the above expressions.

$$b = 0.096/3 = 0.032 \text{ atm}$$

$$a = \frac{9 \times 0.032}{2}(0.0821 \times 150 - 2 \times 0.032 \times 48) = 1.331 \text{ atm dm}^6 \text{ mol}^{-2}$$

[60%]

Thermodynamic integration can be used to find the change in Helmholtz free energy if the system pressure is known as function of the volume. From the master equation for Helmholtz free energy:

$$\mathrm{d}F = -S\mathrm{d}T - p\mathrm{d}V \Rightarrow p = -\left(\frac{\partial F}{\partial V}\right)_{NT} \therefore \Delta F = -\int_{V_1}^{V_2} p\mathrm{d}V$$

In this case, the parameterised van der Waals equation of state can be used to find the free energy change, as follows:

$$\Delta F = -\int_{V_1}^{V_2} p\mathrm{d}V = -\int_{V_1}^{V_2} \left\{\frac{RT}{(V_m - b)} - \frac{a}{V_m^2}\right\}\mathrm{d}V_m = \left[\frac{a}{V_m} + RT\ln(V_m - b)\right]_{V_2}^{V_1}$$

$$= a\left(\frac{1}{V_1} - \frac{1}{V_2}\right) - RT\ln\left[\frac{V_2 - b}{V_1 - b}\right]$$

$$= 1.331 \times \left(\frac{1}{0.0650} - \frac{1}{0.1351}\right) - 0.0821 \times 150 \times \ln\left[\frac{0.1351 - 0.032}{0.0650 - 0.032}\right]$$

$$= -3.404 \text{ dm}^3 \text{ atm mol}^{-1}$$

$$= -344.9 \text{ J mol}^{-1}$$

[30%]

7.

Assumptions: Spherical cluster approximation (cluster is a sphere)
Liquid bulk density inside and vapour pressure outside

Vapour to bulk liquid:
(Favoured)

$$= (\mu_l - \mu_S)n$$

$$= -nk_BT\ln(\frac{P}{P_e})$$

$$= -nk_BT\ln(S)$$

Formation of a surface
(Unfavoured)

$$= \sigma A$$

$$= \sigma 4\pi\left(\frac{3V}{4\pi}\right)^{2/3} n^{2/3}$$

$$\boxed{\Delta G = -nk_BT\ln(S) + \sigma 4\pi\left(\frac{3V}{4\pi}\right)^{2/3} n^{2/3}}$$

[20%]

(a)

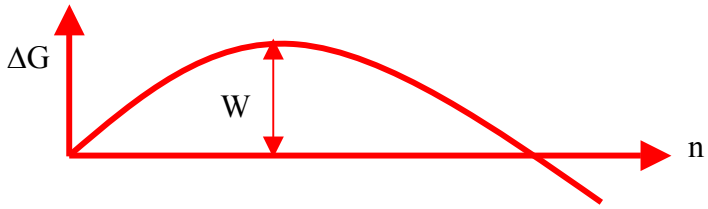

Differentiate ΔG and set equal to zero to obtain the maximum point.

$$\frac{d\Delta G}{dn} = 0$$

$$n^* = \frac{32\pi\sigma^3 V^2}{3(k_BT\ln S)^3}$$

Hence, $n^* = \dfrac{32\times\pi\times 1.8^3\times(1.4\times10^{-29})^2}{3\left(1.38\times10^{-23}\times1400\times\ln 100\right)^3} = 54.4$

For clusters with fewer than n* atoms, the energy cost of making the surface is higher the energy saving of forming a bulk liquid.

[30%]

(b)

The two elements have fundamentally different bonding (silicon bonds covalently, while Au bonds metallically) so they cannot form a single-phase solid solution by substitution of one element for another in the crystal lattice (immiscible, no solubility).

(i) L
(ii) L + Au
(iii) Au + Si
(iv) L + Si

[15%]

(c)

The vapour-liquid-solid (VLS) process for nanowire growth can be described as follows, referring to a schematic plot of phase diagram:

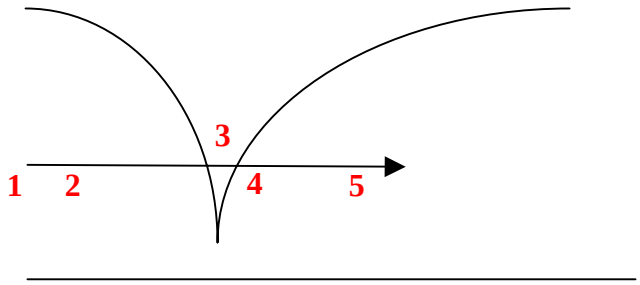

1. Pure gold particle
2. Feed gas breaks down on gold and Si enters gold particle. Gold particle melts to form (L + Au)
3. More Si arrives at particle and the particles become molten alloy (L)
4. Bi-phasic region – Si begins to precipitate out of the droplet at the droplet-substrate interface
5. Precipitation continues at existing interface

[20%]

(d) 360°C (eutectic temperature)

Diameter is controlled by gold particle size/templating in pores
Length is controlled by reaction time.

[15%]